A Linear-Switched Observer for Large-Signal State Estimation in Power Electronics

Jason Poon*, Adrien Genić*, Xiangyu Ding†, Alejandro Domínguez-García†, Ivan Čelanović*

*Massachusetts Institute of Technology, Cambridge, MA 02139, USA
{jsn, adrieng, ivanc}@mit.edu

†University of Illinois at Urbana-Champaign, Urbana, IL 61801, USA
{ding3, aledan}@illinois.edu

Abstract—In this paper, we describe the design and implementation of a state observer for power electronics converters, the dynamics of which can be described by a linear-switched state-space model. The observer is also described by a linear-switched state-space model, and for each particular subsystem, the observer essentially behaves as a Luenberger observer. As part of the design procedure, we provide sufficient conditions that guarantee the stability of the observer. In order to experimentally demonstrate its feasibility, the observer is implemented in a dedicated real-time processor architecture. We present experimental results that illustrate the observer behavior when used for state estimation in single-phase and two-phase boost converters.

I. INTRODUCTION

A state observer can be loosely defined as a causal filter that enables the estimation of certain variables of interest in a physical system. In the context of linear time-invariant (LTI) systems described by a state-space model, a type of observer known as the Luenberger observer (see, e.g., [1]) can be constructed by adding a feedback term to the state-space model. Under certain observability conditions, by appropriately choosing the feedback gain, the observer asymptotically estimates the actual system states.

In power electronics converters, it is common to use small-signal (linearized) average models for control design purposes (see, e.g., [2]). The use of these linearized average models for designing a Luenberger observer appears to be an appealing solution for state estimation in power electronics; however, such a solution would only capture the average behavior of the converter variables, neglecting dynamic effects that are inherent to the converter switching behavior, e.g., voltage and current ripple. On the other hand, there is a large class of power electronics converters for which such large-signal behavior can be accurately described by a linear-switched state-space model; the reader is referred to [3] for an overview on switched system modeling and analysis. In this paper, we consider power electronics converters within such a class and develop state observers for these types of systems. In this regard, we essentially adopt the same linear-switched observer structure as in [4]. Additionally, we demonstrate their feasibility in actual applications, by implementing them on an application-specific real-time processor.

Loosely speaking, a linear-switched observer is comprised of a collection of linear state-space models (subsystems), each of which has the same structure as a Luenberger observer, including the corresponding gain matrix. The transitions between the subsystems are determined by the same rules that govern the switching in the actual system; thus, a challenge is to provide a computational platform that can execute the observer in real-time. Another challenge is to design the individual gain matrices so that the observer is stable. With respect to this, it is well-known that choosing the individual gains such that each subsystem is stable is not sufficient for ensuring stability (see, e.g., [3]). Thus, as part of the observer design procedure, we provide sufficient conditions that ensure the choice of gain matrices renders the observer stable.

In order to experimentally demonstrate the feasibility of the proposed observer, we provide experimental results that involve single-phase and two-phase (interleaved) boost converters with switching frequencies on the order of 10 kHz; the accuracy of the estimates is verified by comparison with actual measurements. In this regard, in order to realize an observer for these converters, we need to, essentially, run *in real-time*, a copy of the linear-switched state-space model describing the converter (including the transitions among the subsystems). In order to achieve this, we rely on an application-specific processor architecture, tailored for low-latency execution of linear-switched state-space models [5], [6]. This computational platform enables the simulation of such models (tailored to power electronics applications) with a fixed 1 μs simulation time step, including input-output latency, and guarantees the computation time for each time step to be shorter than the fixed simulation time step. It is worth noting that, in other existing platforms [7]–[9], the simulation time step is limited by a sampling time between 10 and 50 μs.

The remainder of the paper is organized as follows. Section II presents the observer design procedure and provides practical considerations for implementation in a real-time setting. Section III describes the hardware testbed used to verify the feasibility of the proposed observer, while Section IV presents experimental results for single- and two-phase boost converters. Concluding remarks are presented in Section V.
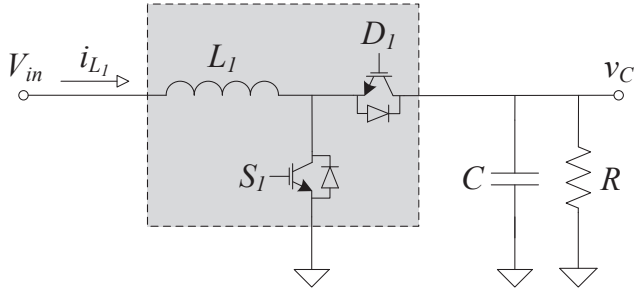
Fig. 1. Single-phase boost converter topology.

II. OBSERVER DESIGN AND IMPLEMENTATION

In this section, we develop an observer for the class of power electronics converters that can be described by a linear-switched state-space model. we provide some considerations for practical implementation in order to enable the execution of the observer in a real-time processor.

A. System Model

A power electronics converter can be thought of as a *switched system*, i.e., a continuous-time system with discrete (isolated) switching events, and (in general), its dynamics can be described by a linear-switched state-space model (see, e.g., [3]) of the form

$$\dot{x}(t) = A_{\sigma(t)}x + B_{\sigma(t)}u(t), \qquad (1)$$

where $x(t) \in \mathbb{R}^n$ is the vector of state variables, and $u(t) \in \mathbb{R}^m$ is the vector of system inputs; the function $\sigma : [0, \infty) \rightarrow \mathcal{Q}$, called the switching signal[1], indicates the active subsystem at every time; $\mathcal{Q}$ is called the "index set", and A_q, B_q, with $q \in \mathcal{Q}$, define the subsystems in (1). To complete the above description, we can add an observation equation of the form

$$y(t) = Cx(t), \qquad (2)$$

where C is a full-rank $n \times n$ matrix describing the states (or linear combinations thereof) that are available for feedback control.

Example 1: To illustrate the ideas above, consider the boost converter in Fig. 1. The index set $\mathcal{Q}$ can be obtained by all possible open/closed switch combinations of S_1 and D_1, which means there are 4 possible subsystems. However, if we consider the continuous conduction mode (CCM) of operation, then only one switch can be closed at any given time. As shown in Table I, this results in only two feasible subsystems (0 indicates that a switch is open and 1 that a switch is closed).

[1]A switching signal, as defined in [3], is a piecewise constant and every-where right-continuous function that has a finite number of discontinuities t_i, which we call *switching times*, on every bounded time interval and thus $\sigma(t) = q \in \mathcal{Q}, \forall t \in [t_i, t_{i+1})$.

TABLE I
FEASIBLE SUBSYSTEMS FOR BOOST CONVERTER IN CCM

q	1	2
S_1	1	0
D_1	0	1

Then, following the notation in (1), we have that $x(t) = [i_{L_1}(t), v_C(t)]^T$, $u(t) = V_{in}$, $\mathcal{Q} = \{1, 2\}$, with

$$A_1 = \begin{bmatrix} 0 & 0 \\ -\frac{1}{RC} & 0 \end{bmatrix}, \qquad B_1 = \begin{bmatrix} \frac{1}{L_1} \\ 0 \end{bmatrix},$$

$$A_2 = \begin{bmatrix} 0 & -\frac{1}{L_1} \\ \frac{1}{C} & -\frac{1}{RC} \end{bmatrix}, \qquad B_2 = \begin{bmatrix} \frac{1}{L_1} \\ 0 \end{bmatrix}.$$

Additionally, assuming that both $i_{L_1}(t)$ and $v_C(t)$ are available for feedback control, we have that C is the 2×2 identity matrix. □

B. Observer Design

Consider the linear-switched system in (1) and denote by $\hat{x}(t)$ an estimate of the state vector $x(t)$. The objective is to design a causal filter that takes $u(t)$, $y(t)$, and $\sigma(t)$ as inputs and generates a residual $\gamma(t) := y(t) - C\hat{x}(t)$ such that $\lim_{t \to \infty} \gamma(t) = 0$. Following the concepts presented in [4], we consider filters of the form

$$\dot{\hat{x}}(t) = A_{\sigma(t)}\hat{x}(t) + B_{\sigma(t)}u(t) + L_{\sigma(t)}\gamma(t), \qquad (3)$$

$$\gamma(t) = y(t) - C\hat{x}(t),$$

where $\sigma(t)$, $A_{\sigma(t)}$, $B_{\sigma(t)}$, $q \in \mathcal{Q}$ and C as in (1); and

$$L_{\sigma(t)} = [\mu I_n + A_\sigma(t)] C^{-1}, \ \forall t, \qquad (4)$$

for some $\mu > 0$ (I_n denotes the $n \times n$ identity matrix). Next, we establish that with the choice of $L_{\sigma(t)}$ in (4), we have that (3) is stable and $\lim_{t \to \infty} \gamma(t) = 0$. From (3) and (4), it follows that

$$\dot{\hat{x}}(t) = -\mu\hat{x}(t) + B_{\sigma(t)}u(t) + [\mu I_n + A_\sigma(t)]x(t) \qquad (5)$$

This is a linear time-invariant system, which is stable since $\mu > 0$. Now, let $e(t) := x(t) - \hat{x}(t)$. By subtracting (3) from (1), we obtain that

$$\frac{de(t)}{dt} = [A - L_{\sigma(t)}C] e(t),$$

With the choice of $L_{\sigma(t)}$ in (4), we have that

$$\frac{de(t)}{dt} = -\mu e(t),$$

$$\gamma(t) = Ce(t),$$

for some $\mu > 0$, from where we obtain that $\lim_{t \to \infty} \gamma(t) = 0$.

Example 2: Consider again the boost converter in Fig. 1 and assume as before that C is the 2×2 identity matrix; then, following the notation in (4), we have that

$$L_1 = \begin{bmatrix} \mu & 0 \\ -\frac{1}{RC} & \mu \end{bmatrix}, \quad L_2 = \begin{bmatrix} \mu & -\frac{1}{L_1} \\ \frac{1}{C} & \mu - \frac{1}{RC} \end{bmatrix}.$$

for some $\mu > 0$. □

C. Observer Implementation

From (3), one can see that in order to execute the linear observer, we essentially need to run a copy of the system in (1) in real-time. To accomplish this, we use the processor platform described in [6]. In particular, given (1), this processor platform simulates discrete-time linear-switched models of the form

$$x_{k+1} = A_{d_{\sigma(t)}} x_k + B_{d_{\sigma(t)}} u_k, \tag{6}$$

where $A_{d_{\sigma(t)}}$ and $B_{d_{\sigma(t)}}$ result from discretizing the continuous state-space matrices $A_{\sigma(t)}$ and $B_{\sigma(t)}$, respectively. Thus, in order to execute the observer in (3) on the processor platform, we need to obtain a discrete-time model of the form in (6).

Define $u^* = [u^T, \ y^T]^T$, then we can rewrite (3) as

$$\dot{\hat{x}}(t) = A^*_{\sigma(t)} \hat{x}(t) + B^*_{\sigma(t)} u^*(t)$$

where

$$A^*_{\sigma(t)} = A_{\sigma(t)} - L_{\sigma(t)} C = -\mu I_n,$$

$$B^*_{\sigma(t)} = \begin{bmatrix} B_{\sigma(t)} & \mu I_n + A_{\sigma(t)} \end{bmatrix} \tag{7}$$

Now, from (7), we can obtain a discrete-time model of the form in (6) by defining

$$A^*_{d_{\sigma(t)}} = e^{-\mu h} I_n, \tag{8}$$

$$B^*_{d_{\sigma(t)}} = \int_0^h e^{-\mu t} B^*_{\sigma(t)} \, \mathrm{d}t, \tag{9}$$

where h is the fixed time step. Then, by solving the integral in (9), we obtain that

$$B^*_{d_{\sigma(t)}} = \frac{1}{\mu}(e^{-\mu h} - 1) B^*_{\sigma(t)}. \tag{10}$$

Thus, the system state estimate $\hat{x}_{k+1}$ and estimated output $\hat{y}_k$ can be computed as:

$$\hat{x}_{k+1} = A^*_{d_{\sigma(t)}} \hat{x}_k + B^*_{d_{\sigma(t)}} u^*_k \tag{11}$$

$$\hat{y}_k = C \hat{x}_k$$

A linear solver computes the system state estimate based on (11). An internal signal generator and external analog input ports provide the input u^*_k to the state-space solver. The system state estimate $\hat{x}_k$ and the estimated output $\hat{y}_k$ are accessible in real-time through low-latency analog output ports. During real-time execution, a direct memory indexing technique controls the selection of the mode of the system based on inputs
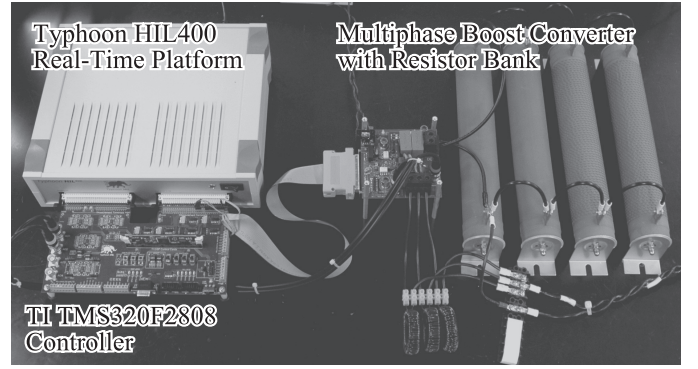
(a) Picture of the hardware testbed. The controller and real-time processor are shown on the left, and the power electronics converter system is shown on the right.
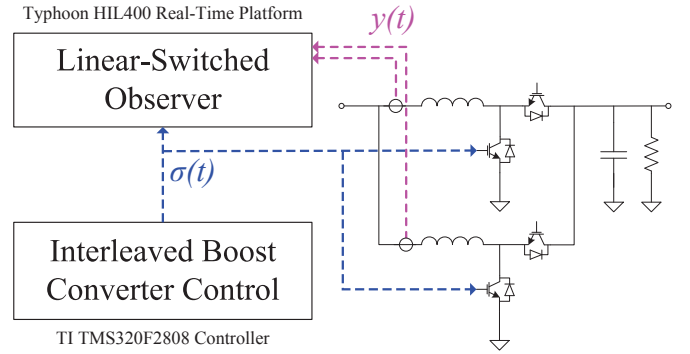
(b) Diagram of the hardware testbed for the two-phase interleaved boost converter topology. As seen, the controller provides the switching signal $\sigma(t)$ and the observer measures i_{L_1} and i_{L_2} from the physical plant.

Fig. 2. Hardware testbed.

u^*_k to the system and boundary conditions dependent on the system state estimate $\hat{x}_k$. Each mode q defines a set of state-space matrices A^*_q and B^*_q that are computed on the linear solver. The processor architecture, which is implemented in a field-programmable gate array (FPGA) device, guarantees the duration of execution for each time interval to be shorter than the fixed time step h, resulting in real-time performance regardless of the system size. Furthermore, the loop-back latency is minimized with custom designed input-output hardware, and has been characterized to be on the order of 1 μs.

III. HARDWARE TESTBED

In this section, we describe the hardware setting used to experimental demonstrate the proposed linear-switched observer for power electronics converters. Specifically, we focus on single-phase and two-phase (interleaved) boost converters. The complete hardware setup is shown in Fig. 2a. As seen in the figure, there are three main components: (i) a digital controller, (ii) a power electronics converter, and (iii) a real-time platform; next, we describe each of these components.

The control platform chosen for this hardware setup is the Texas Instruments (TI) TMS32012808. A custom interface PCB was designed in order to send open-loop gate drive signals to both the real-time platform and the power electronics converter.
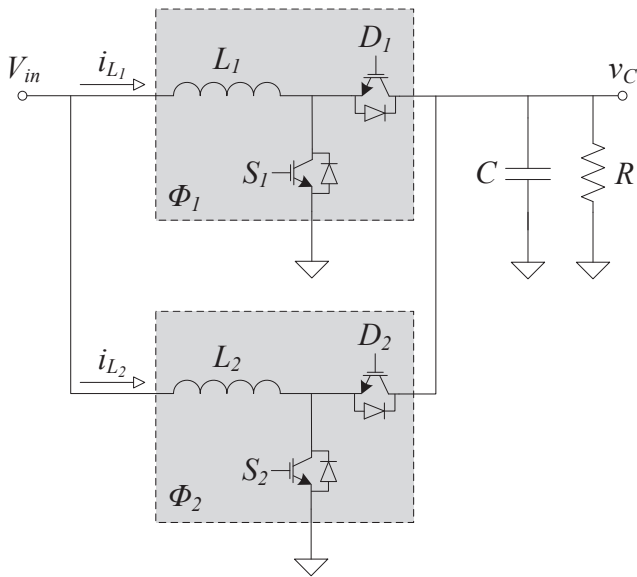
Fig. 3. Two-phase boost converter topology.

TABLE II
COMPONENT VALUES FOR THE MULTIPHASE BOOST CONVERTER SETUP.

V_{in}	50 Vdc
$L_{1,2}$	650 nH
C	4.4 μF
R	38.1 Ω
Switching frequency	8 kHz
Duty cycle	0.5

The power electronics converter used in the hardware testbed is a two-level, three-phase inverter wired in a three-phase boost converter configuration. For the results presented in this paper, we only operate the single-phase and two-phase (interleaved) boost converter configurations; the phases that are unused are disconnected during operation. Figures. 1 and 3 show the schematic diagrams and component naming conventions of both topologies. Component values for both topologies and the controller are shown in Table II. The linear-switched state-space model for the single-phase configuration was derived in Example 1; the model for the two-phase configuration can be derived in a similar fashion and therefore is omitted.

The real-time platform chosen for this hardware setup is the Typhoon HIL400 [10], [11]. The HIL400 is a commercial off-the-shelf real-time processor architecture that implements the ideas described in Section II-C. The HIL400 is an integrated system that provides low latency analog and digital input/output ports and a FPGA processor that runs the linear solver architecture. The real-time platform is used to execute, in real-time (with $h = 1$ μs), the observers for both the single- and two-phase (interleaved) boost converters. For each topology, measured state variables from the converter, such as inductor currents, are sent to the real-time platform through low-latency analog input ports. The system state estimate can be obtained directly from the real-time platform through analog output ports.

IV. EXPERIMENTAL RESULTS

Using the experimental setup described in Section III, we demonstrate the feasibility of the proposed observers to estimate, in real-time, the states of the single-phase and two-phase boost (interleaved) converters. In all experiments, in order to compare the accuracy of the observer, we compare the system state states with measurements of the actual system states.

A. Single-phase boost converter observer

In the first experiment, the observer is used to estimate the full system state of a single-phase boost converter. The current through the inductor L_1, $i_{L_1}(t)$, is measured by the observer. The observer estimates the full system state, $\hat{x}(t) = \left[\hat{i}_{L_1}, \hat{v}_C\right]^T$.

Figures. 4a and 4b show a comparison between the estimated full system state from the observer and the measured system state from the boost converter. As the figures show, the estimates for both system states, as provided by the observer, closely match the corresponding measurements of both system states $i_{L_1}(t)$ and $v_C(t)$. The observer accurately estimates the ripple in both state variables that occurs on the time scale of the switching frequency (8 kHz).

B. Two-phase (interleaved) boost converter observer

In the second experiment, the observer is used to estimate the full system state of a two-phase (interleaved) boost converter. The currents through the inductor L_1 and L_2, $i_{L_1}(t)$ and $i_{L_2}(t)$, respectively, are measured by the observer. The observer reconstructs an estimation of the full system state, $\hat{x}(t) = \left[\hat{i}_{L_1}, \hat{i}_{L_2}, \hat{v}_C\right]^T$.

Figures. 5a and 5b show a comparison between the estimated full system state, as provided by the observer, and the corresponding state measurements. As shown in both figures, the system state estimates closely match the corresponding measurements of the converter system states $i_{L_1}(t)$, $i_{L_2}(t)$, and $v_C(t)$.

V. CONCLUDING REMARKS

In this paper, we described the design and implementation of a state observer for power electronics converters. Our experimental results demonstrated the feasibility of executing this observers in real-time for switching frequencies up to 10 kHz. While the single-phase and two-phase (interleaved) boost converters are used as an application example, the design technique and implementation is applicable to a wider class of power electronics converters that can be described with a linear-switched state-space model.
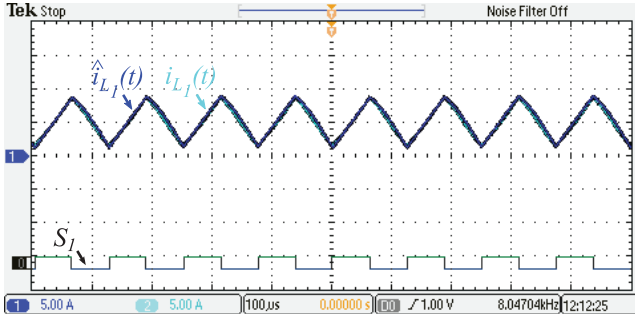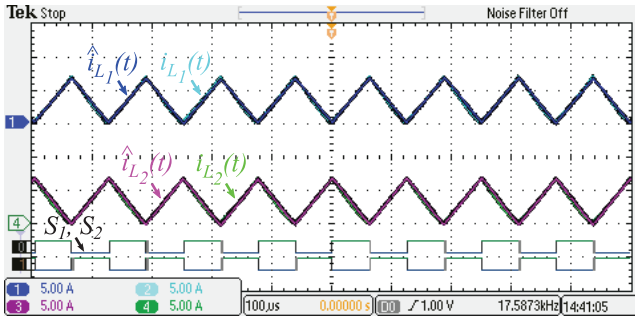
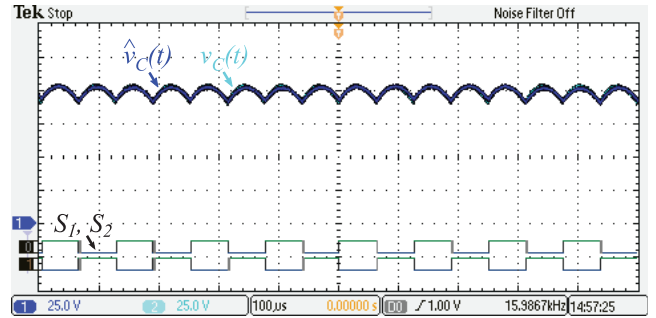(a) Comparison between estimated state $\hat{i}_{L_1}(t)$ (blue) and measured state $i_{L_1}(t)$ (cyan).
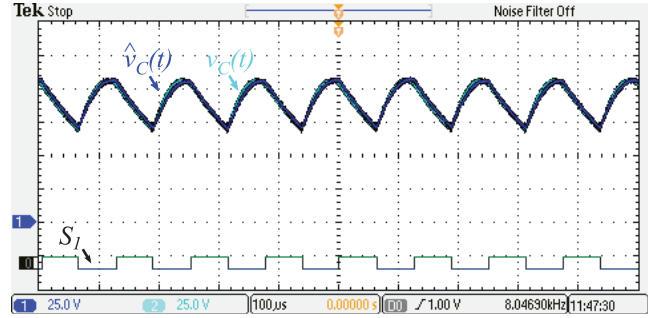
(b) Comparison between estimated state $\hat{v}_C(t)$ (blue) and measured state $v_C(t)$ (cyan).

Fig. 4. Observer-based system state estimation for single-phase boost converter.

(a) Comparison between estimated states $\hat{i}_{L_1}(t)$ (blue) and $\hat{i}_{L_2}(t)$ (magenta) and measured states $i_{L_1}(t)$ (cyan) and $i_{L_2}(t)$ (green).

(b) Comparison between estimated state $\hat{v}_C(t)$ (blue) and measured state $v_C(t)$ (cyan).

Fig. 5. Observer-based system state estimation for two-phase (interleaved) boost converter.

REFERENCES

[1] D. G. Luenberger, "Observing the state of a linear system," *IEEE Transactions on Military Electronics*, vol. 8, no. 2, pp. 74–80, 1964.

[2] J. Kassakian, M. Schlecht, and G. Verghese, *Principles of Power Electronics*. Reading, MA: Addison-Wesley, 1991.

[3] D. Liberzon, *Switching in Systems and Control*. Boston, MA: Birkhauser, 2003.

[4] A. Alessandri and P. Coletta, "Design of Luenberger observers for a class of hybrid linear systems," in *Proc. Hybrid Systems Computation and Control*, (Genova, Italy), 2001.

[5] D. Majstorovic, Z. Pele, A. Kovacevic, and N. Celanovic, "Computer based emulation of power electronics hardware," in *Proc. First IEEE Eastern European Conf. the Engineering of Computer Based Systems ECBS-EERC '09*, pp. 56–64, 2009.

[6] D. Majstorovic, I. Celanovic, N. Teslic, N. Celanovic, and V. Katic, "Ultra-low latency hardware-in-the-loop platform for rapid validation of power electronics designs," *IEEE Transactions on Industrial Electronics*, no. 99, 2011.

[7] J. Wu, C. Dufour, and L. Sun, "Hardware-in-the-loop testing of hybrid vehicle motor drives at Ford Motor Company," in *Proc. IEEE Vehicle Power and Propulsion Conf. (VPPC)*, pp. 1–5, 2010.

[8] M. Harakawa, C. Dufour, S. Nishimura, and T. Nagano, "Real-time simulation of a PMSM drive in faulty modes with validation against an actual drive system," in *Proc. 13th European Conf. Power Electronics and Applications EPE '09*, pp. 1–9, 2009.

[9] A.-L. Allegre, A. Bouscayrol, J.-N. Verhille, P. Delarue, E. Chattot, and S. El-Fassi, "Reduced-scale-power hardware-in-the-loop simulation of an innovative subway," *IEEE Transactions on Industrial Electronics*, vol. 57, no. 4, pp. 1175–1185, 2010.

[10] M. Vekic, S. Grabic, D. Majstorovic, I. Celanovic, N. Celanovic, and V. Katic, "Ultra low latency HIL platform for rapid development of complex power electronics systems," *IEEE Transactions on Power Electronics*, 2012. Early Access.

[11] N. L. Celanovic, I. L. Celanovic, and Z. R. Ivanovic, "Cyber physical systems: A new approach to power electronics simulation, control and testing," *Advances in Electrical and Computer Engineering*, vol. 12, no. 1, pp. 33–38, 2012.